Emissions and performance with diesel and waste lubricating oil : a fundamental study into cold start operation with a special focus on particle number size distribution

Zare, A, Bodisco, T, Verma, P, Jafari, M, Babaie, M, Yang, L, Rahman, MM, Banks, A, Ristovski, Z, Brown, RJ and Stevanovic, S

http://dx.doi.org/10.1016/j.enconman.2020.112604

Emissions and performance with diesel and waste lubricating oil: A fundamental study into cold start operation with a special focus on particle number size distribution

Ali Zare[a,*], Timothy A. Bodisco[a], Puneet Verma[b,c], Mohammad Jafari[b,c], Meisam Babaie[d], Liping Yang[e], M.M Rahman[f], Andrew Banks[g], Zoran D. Ristovski[b,c], Richard J. Brown[b], Svetlana Stevanovic[a]

[a] Flow, Aerosols & Thermal Energy (FATE) Group, School of Engineering, Deakin University, VIC, 3216 Australia

[b] Biofuel Engine Research Facility, Queensland University of Technology (QUT), QLD, 4000 Australia

[c] International Laboratory for Air Quality and Health, Queensland University of Technology (QUT), QLD, 4000 Australia

[d] School of Computing, Science and Engineering (CSE), University of Salford, Salford, Manchester M5 4WT, United Kingdom

[e] Institute of Power and Energy Engineering, Harbin Engineering University, No. 145-1, Nantong Street, Nangang District, Harbin, 150001, China

[f] School of Mechanical Aerospace and Automotive Engineering, Coventry University, Coventry CV1 2JH, UK

[g] Queensland Alliance for Environmental Health Sciences, The University of Queensland, , QLD, 4072 Australia

Abstract

This study investigates the effect of engine temperature during cold start and hot start engine operation on particulate matter emissions and engine performance parameters. In addition to a fundamental study on cold start operation and the effect of lubricating oil during combustion, this research introduces important knowledge about regulated particulate number emissions and particulate size distribution during cold start, which is an emerging area in the literature. A further aspect of this work is to introduce waste lubricating oil as a fuel. By using diesel and two blends of diesel with 1 and 5% waste lubricating oil in a 6-cylinder turbocharged engine on a cold start custom test, this investigation studied particle number (PN), friction losses and combustion instability with diesel and waste lubricating oil fuel blends. In order to understand and explain the results the following were also studied: particle size distribution and median diameter, engine oil, coolant and exhaust gas temperatures, start of injection, friction mean effective pressure (FMEP), mechanical efficiency, coefficient of variation (CoV) of engine speed, CoV of indicated mean effective pressure (IMEP) and maximum rate of pressure rise were also studied. The results showed that during cold start the increase in engine temperature was associated with an increase in PN and size of particles, and a decrease in FMEP and maximum rate of pressure rise. Compared to a warmed up engine, during cold start, PN, start of injection and mechanical efficiency were lower; while FMEP, CoV of IMEP and maximum rate of pressure rise were higher. Adding 5% waste lubricating oil to the fuel was associated with a decrease in PN (during cold start), decreased particle size, maximum rate of pressure rise and CoV of IMEP and was associated with an increase in PN and nucleation mode particles (during hot start) and FMEP.

Keywords: Cold-start; engine warm up; waste lubriacating oil; Particulate matter; PN; particle size distribution.

1. Introduction

There are a number of studies in the literature on using waste materials as a fuel instead of fossil fuels [1-5], owing to some negative aspects of using fossil fuels such as environmental aspects, cost and their depletion [6], and also due to the fact that some alternative fuels from wastes can improve the engine emission and performance parameters [7]. For example, Amid et al. [8] investigated the effects of waste-derived ethylene glycol diacetate on performance and emission characteristics of a diesel engine fueled with diesel/biodiesel blends and reported that the selected fuel blends could significantly mitigate carbon dioxide emission; however, NOx and unburned hydrocarbons increased and it also negatively affected engine performance parameters such as fuel consumption and thermal efficiency. Verma et al. [9] investigated the possibility of using waste tyre oil as a fuel in internal combustion engines looking at engine performance and emissions parameters and reported that it adversely affected the thermal efficiency and fuel consumption and increases the CO and HC. It has been reported that using waste cooking oil as a fuel can reduce particulate matter emissions. Nabi et al. [10] used biodiesel derived from waste cooking oil as a fuel in a diesel engine and reported a substantial reduction in particulate matter emissions (maximum 88% in PN and 84% in PM). Using waste cooking oil derived biodiesel (due to its fuel oxygen content) was also reported to be the reason for a reduction in PM and PN emissions under steady-state [11] and transient engine operations [12]. In terms of engine performance parameters, Zare et al. [13] reported that using 100% biodiesel derived from waste cooking oil can increase the thermal efficiency and decrease the friction power in a diesel engine. Another example of using waste material as a fuel in a diesel engine could be the use of triacetin as a fuel additive which led to a significant reduction in PM and PN emissions [14, 15].

This study also introduces the waste lubricating oil as a fuel. Between waste materials, lubricating oil represents 60% of residual oils which are produced massively every year

worldwide (24 million tonnes/year) [16]. Given the amount produced every year and the availability, waste lubricating oil can potentially be used as a fuel, however, the effect of using such a fuel needs to be investigated under different engine operating conditions such as cold start.

It is common for many vehicles to be started in the morning when it is cold, driven from home to work, parked for some hours, started in the afternoon when it is again cold, driven back home and then parked overnight. In cities, this is the daily norm for the majority of vehicles [17] and many trips start and finish before the engine fully warms up [18]. A studying on 55 vehicles over 1000 trips (71000 km with the total duration of 1260 hours) showed that one third of the trips occurred within cold start [17]. Modelling of excess emissions during cold start in a study, which used the data of 1,766 passenger cars (35,941 measurements) estimated 5.2 km to be the average cold start distance in which the exhaust emissions stabilise [19].

Cold start can be defined from the engine start either for 5 minutes or until the engine coolant temperature reaches 70 degC (EU Directive 2012/46/EU). During cold start the engine temperature is not optimal, which can adversely affect the engine performance parameters such as fuel consumption and thermal efficiency [20], and emission parameters such as NOx [21]. One of the reasons is the sub-optimal temperature of the cylinder walls and engine block. For example, Robert et al. [22] reported that the low temperature of the cylinder wall increased the emissions and also impacted fuel economy. A study by Cao [23] showed that the low temperature of the engine block caused incomplete combustion and therefore could be attributed to increased emissions. During cold start, the low temperature of the fuel and engine can also impact the fuel atomisation and evaporation process, which also adversely affect engine performance and emissions [24].

Cold start emissions have been reported to be a significant portion of the total emissions [18, 25]. For example, around 30% of the total PM from the LA92 Unified Driving Cycle was related to Phase 1, which represents only 12% of the total distance in that cycle. Also comparing Phase 1, which was cold start, to Phase 3, where the engine was hot, showed that the PM from Phase 1 was 7.5 times higher than from Phase 3 [26]. Bielaczyc et al. [27] reported that PM emissions from the first three minutes of cold start were much higher than that of hot start contributing more than 40% of the total emissions. Another study used the FTP test cycle and showed that cold start NOx emissions can be up to two times higher than those of hot start [28].

Cold start operation affects the engine performance as well [29, 30]. Increased friction losses and decreased thermal efficiency were also the result of sub-optimal engine temperature. This is because during cold start, the viscosity of the engine lubricating oil is higher than during hot start [22, 31]. Will and Boretti [32] reported 2.5 times higher friction losses during cold start when compared to hot start. The higher friction losses during cold start leads to higher fuel consumption. A study by Samhaber et al. [33] showed a 13.5% increase in fuel consumption as a result of cold start, when compared to hot start. Zare et al. [20] showed that during cold start the indicated torque, fuel consumption, engine instability and friction losses are higher than during hot start.

The literature states that the efficiency of after-treatment systems during cold start is one of the main reasons for higher emissions [22]. While understanding the impact of cold start on after-treatment is critically important, there is also a need for fundamental studies showing how the engine temperature can be influential on the feedgas emissions. Currently, there is no fundamental study in the literature investigating how a transient increasing engine temperature influences the total concentration of particles and also the size of particles during cold start at constant engine load and speed. The current work here will investigate this.

Most of the literature on cold start operation used a driving cycle which includes the cold start section at the start. Given that driving cycles are characterised by various speed and load changes, cold start emissions and performance within cycles are significantly influenced by such changes, which consequently affects the fuel injection strategy and other engine parameters [34]. Given that under different operating conditions, the engine performance and emission parameters can be affected by different factors reinforcing or cancelling the effect of one another, having different variables over a cycle when it comes to data analysis can limit the fundamental study into the pure effect of engine temperature change. In most of the literature, cold start data is presented as an average value over the cold start section, which limits the value of the study given that cold start has different stages, which will be discussed and addressed in this study.

Outside of the fundamental cold start investigation, this study looks into the effect of lubricating oil which exists inside the cylinder during combustion. It is reported in the literature that the presence of lubricating oil in addition to the injected fuel during combustion can influence engine performance and emissions [35]. This study artificially adds lubricating oil into the cylinder with the fuel through blending, therefore facilitating a study into the effect of lubricating oil on engine performance parameters (such as mechanical efficiency and combustion stability) and exhaust emissions (such as PN and PN size distribution). This study is significantly important from the particle size distribution point of view given that smaller particles are more toxic [36]. The current literature has related some small particles to the existence of lubricating oil during combustion [35]. Presently, the authors were not able find a fundamental study in the literature looking at the effect of engine lubricating oil on PN and PN size distribution during cold start.

This study serves as a reference for engine researchers and car manufacturers when it comes to new emissions regulations, in which, in addition to PN, the size of the particles will also be

important. In the most recent European emissions regulation, Euro 6.2, the current method which is called the particle measuring program (PMP), only considers solid particles with a size above 23 nm [37]. However, for the upcoming regulation, there is a plan to include sub-23 nm particles in the PN measurement [38]. Currently, different research groups are working on that. For example, the SUREAL-23 project received funding from the European Union's Horizon 2020 research and innovation programme under grant agreement No 724136 to work on sub-23 nm particles. Therefore, this study is of importance given that the existence of lubricating oil in the combustion significantly affects the sub-23 nm particles.

In the literature, there are some studies evaluating waste lubricating oil as a fuel [32, 35, 39-41]. However, the authors could not find any study investigating the influence of using this fuel on PN, PN size distribution, friction losses and combustion instability parameters during different stages of cold start in comparison to hot start; cold start operation is of significant importance owing to the fact that during this period the after-treatment systems do not perform well.

2. Experimental facilities

2.1 Engine specifications

Meeting the emissions limit of new regulation such as Euro IV-VI forces car manufacturers to use exhaust after-treatment systems such as the Diesel Particulate Filter (DPF) for their new vehicles. With such engines, emissions will be dependent on the type and performance of the after-treatment system, therefore using such engines for research purposes can limit the fundamental study on the pure effect of engine temperature or the fuel properties on engine emissions during cold start, which are the aims of this study. Therefore, in order to gain better insight into the actual engine dependent particulate matter emissions, avoiding the mentioned limitations, it was opted to conduct the experiment on a Euro III engine, as specified in Table

1. The engine in this study was a 6-cylinder turbocharged common-rail diesel engine which was coupled to a hydraulic dynamometer to control the speed and load.

Table 1 Engine specifications

Model	Cummins ISBe220 31
Emission standard	Euro III
Capacity (*l*)	5.9
Aspiration	Turbocharged
Maximum power	162 kW at 2500 rpm
Maximum torque	820 Nm at 1500 rpm
Fuel injection	High pressure common rail
Cylinders	6 in-line
Bore × stroke (mm x mm)	102 × 120
Compression ratio	17.3:1
Dynamometer type	Electronically-controlled water brake dynamometer

2.2 Fuel selection

Apart from D100 (100% diesel), this investigation used 1% (by volume) waste lubricating oil with 99% diesel (D99W1), and 5% waste lubricating oil with 95% diesel (D95W5). The fuel properties of diesel waste lubricating oil are shown in Table 2. A GC/MS instrument (model ISQ, single quadrupole MS, Trace 1310 Gas chromatograph) was used for D100, D99W1 and D95W5 fuel analysis and the analysis result is shown in Table 3. As can be seen, D100 has the highest aromatic and aliphatic compounds and no cyclic hydrocarbons, while D99W1 and D99W5 had cyclic hydrocarbons. Waste lubricating oil and D100 have similar calorific values, therefore the blends with 1 and 5% waste lubricating oil have a similar heating value to D100 [40]. The higher viscosity of the waste lubricating oil can adversely affect the fuel atomisation and evaporation during cold start (owing to the low temperature) which consequently impacts engine performance and emissions parameters [42]. It is known that high sulfur content

192 increases particulate emissions, therefore the higher sulfur content of the lubricating oil can
193 potentially increase the number of particles [35].

194 Given that the current literature has related some small particles to the existence of lubricating
195 oil during combustion [35], artificially adding 1% lubricating oil into the cylinder with the fuel
196 through blending can facilitate the study by highlighting the changes in PN. Using 5% blend
197 can confirm the result and also evaluate the possibility of using it as an alternative fuel.
198 However, due to high viscosity and sulfur content of lubricating oil, it is decided not to use a
199 higher portion of this fuel at this stage.

200

201 Table 2 Diesel and waste lubricating oil properties [40, 43]

	Diesel	Waste lubricating oil
Density (g/cc)	0.84	0.89
Viscosity (mm^2/s)	2.64	30.3
Heating value (MJ/kg)	41.77	43.07
Flash point (degC)	71	98
Sulfur (ppm)	5.9	7500
Ash (ppm)	1	7400

202

203 Table 3 Fuel analysis with GC/MS

	Area%		
	aromatic	aliphatic	cyclic hydrocarbons
D100	1.43-5.66	1-12.24	-
D99W1	0.04-0.10	0.05-0.69	0.07-0.13
D95W5	0.03-0.07	0.03-0.12	0.03-0.07

204

2.3 Design of experiment

There are different methods of running a cold start test. In most of the literature, cold start data is related to the first section of a driving cycle in which the engine coolant temperature is less than 70 degC or the first 5 minutes of the cycle. For example, in WLTC (worldwide harmonised light vehicles test cycle) the cold start section is related to the first 5 minutes of the test or similarly in the NEDC, the urban section contains cold start. According to the aim of this study, which is the evaluation of engine emissions and performance during different stages of cold start and hot start, using a driving cycle may not be effective. The reason is that driving cycles contain frequent speed and load changes (such as ESC, NEDC, WLTC and RDE test route [44, 45]) which adds more effective parameters to the cold start data analysis and makes the judgment more difficult, consequently, it limits the fundamental study into cold start. Therefore, this study uses a constant engine speed of 1500 rpm under 25% load in order to decrease the number of influential parameters aiding a better judgment about the direct effect of engine temperature.

2.4 Test set-up procedure

A schematic diagram of the experimental facility is shown in Figure 1. To measure PN and PN size distribution, this study used a Scanning Mobility Particle Sizer (SMPS) which consists of a TSI 3071A classifier—to preselect particles within a size range, and a TSI 3782 condensation particle counter (CPC)—to grow particles making them optically detectable. During the experiments, raw exhaust gas was diluted with HEPA-filtered ambient air in a dilution tunnel and then directed to the SMPS. In order to calculate the dilution ratio, CO_2 was sampled before the dilution tunnel with a CAI-600 CO_2 (with repeatability > 1% of full scale and linearity > 0.5% of full scale [46]) and after the dilution tunnel with a SABLE CA-10 Carbon CO_2 gas analyser (with an accuracy of 1% of reading within the range of 0-10% [47]). In order to measure the in-cylinder data, a Kistler 6053CC60 piezoelectric transducer (manufactured

stated sensitivity of ≈ -20 pC/bar) was used to measure the in-cylinder pressure, a Kistler type 2614 (manufacture stated resolution= 0.5 crank angle degree) was used to measure the crank angle, the fuel injection signal was directly interrogated by measuring the voltage applied to the first injector. Refs. [48, 49] can provide more information about the experimental facility used in this study.

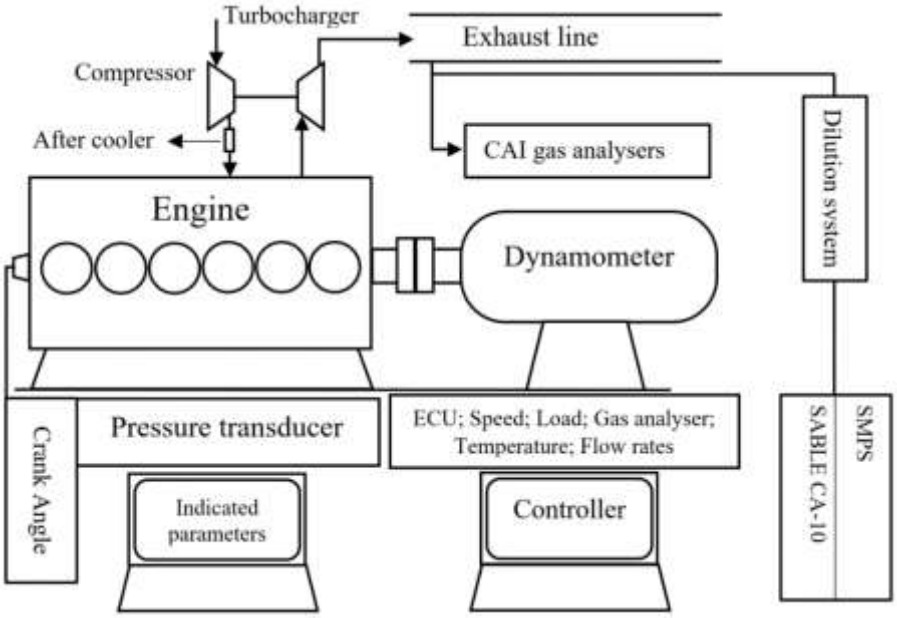

Figure 1 Experimental facility schematic diagram

2.5 Experimental procedure

Cold start tests were conducted every day morning after an overnight (minimum 12 hours) engine-off at ambient temperature. Engine coolant and oil temperatures were checked before each test (temperatures were 23 ± 3 degC). The engine for each test was started at 1500 rpm under a quarter load and ran for at least 30 minutes to fully warm up and stabilise. Before running each test, the engine fuel lines were flushed to make sure there was no leftover fuel from the previous test in the lines.

3. Results and discussion

This section studies PN concentration, and to better explain the observed phenomena, it uses PN size distribution and median diameter and also some of the engine performance parameters such as start of injection and engine oil, coolant and exhaust gas temperatures. This section also studies friction losses using friction mean effective pressure (FMEP) and mechanical efficiency; and the combustion instability using CoV of engine speed and CoV of indicated mean effective pressure (IMEP) supporting the results with the maximum rate of pressure rise data. Results in each sub-section will be analysed from two aspects; the effect of cold start and engine temperature and the effect of fuel properties under different engine operating conditions.

Before moving to the next section, it is worth mentioning about the engine coolant and oil temperature profiles during cold start, which can be the indicators of engine warm up. Figure 2 shows the how the exhaust gas, oil and coolant temperatures change during cold start. As mentioned before, cold start can be defined from the engine start either for 5 minutes or until the engine coolant temperature reaches 70 degC (EU Directive 2012/46/EU). In order to meet the formal definition of cold start, the engine needs to be started after at least 12 hours soak (engine-off) without forced cooling or 6 hours with forced cooling at ambient temperature (EU Directive 2012/46/EU). The definition of cold start in the regulation might give the impression that outside the mentioned boundary, the engine operates as hot start and normal. However, a study by Zare et al. [20] showed that even after the engine coolant temperature reaches 70 degC, the engine still produces sub-optimal exhaust emissions and performance. For example, there is a period in which the engine coolant temperature reached to 70 degC, therefore, it is not cold start anymore; however, the coolant temperature is still sub-optimal and increasing which consequently affects the engine performance and emissions. There can also be another situation in which the engine coolant temperature is optimal, however, the engine oil temperature is still sub-optimal and increasing. The reasons is the lag between the engine

coolant and oil temperatures optimal value [20, 50]. In such a situation the operation is not cold start as per the definition of cold start in EU Directive 2012/46/EU, therefore it is classified as hot start; however, the operation is not yet optimal. As can be seen in Figure 2, when the coolant temperature reaches the steady state value—which consequently leads to the thermostat opening and dissipating heat to the environment through the radiator—the oil temperature is still increasing. This is due to the different temperature rise rate profiles of engine oil and coolant, given that they have different properties [20]. The lag between oil and coolant temperatures to reach the optimal point, which depends on the engine operating condition [20] also has a significant effect on inefficiencies during cold start [51, 52], is not confined to one type of engine [53], and has been frequently reported by other researchers [54-56].

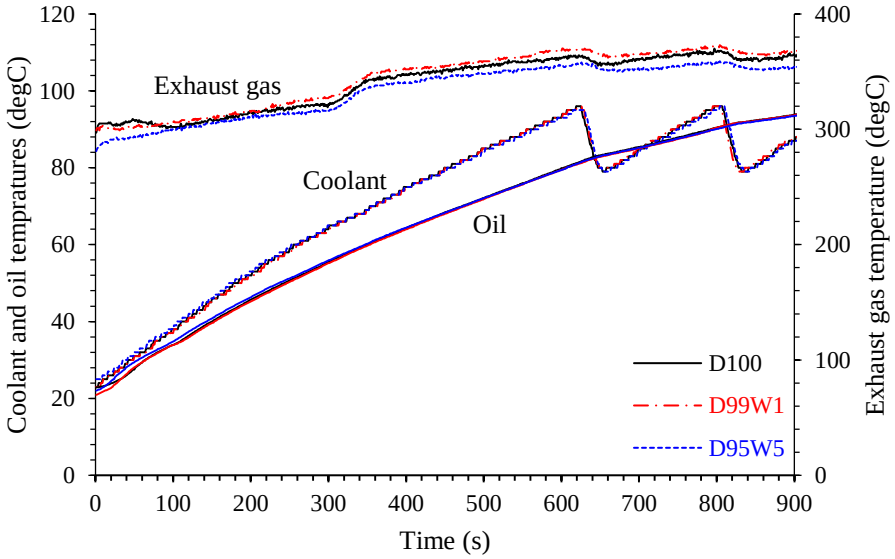

Figure 2 Coolant, oil and exhaust gas temperature within the custom test for all the tested fuels

3.1 Particulate matter

Particulate matter—liquid and solid mixtures in the exhaust gas emissions—is a complicated pollutant which is not a chemically well-defined substance in terms of how it forms, what it is

composed of and how it can be controlled. Particulate matter emissions depend on various factors such as fuel properties, engine speed, engine load, temperature, and after-treatment systems [57]. Particulate matter can negatively impact our ecosystem; it has been recognised as a global risk factor for diseases as small particles are associated with cardiorespiratory health issues [58]. It is also reported that prolonged exposure to particulate matter, which can be associated with reactive oxygen species, can lead to adverse health effects [59-64]. Vaughan et al. [62] studied the effect of organic content from diesel exhaust particles on oxidative stress and inflammation and reported that inflammatory responses may be a key mechanism of response to diesel emissions, more so than oxidative stress. Using an alternative fuel, a study on cytotoxic, inflammatory and oxidative potential caused by engine emissions, Vaughan et al. [64] reported that compared to diesel, using a low fraction of a fuel derived from coconut oil decreased the inflammation and increased antioxidant expression. Stevanovic et al. [59] studied the oxidative potential of combustion emissions and reported that the fuel oxygen content has a positive correlation with the particle phase oxidative potential. A similar result was reported by Hedayat et al. [61] when they studied the effect of fuel oxygen content on particulate oxidative potential using biodiesel.

The count of individual particles, PN, has gained a lot of attention recently as it was recognized that measurement of the particulate mass only is not sufficient and informative enough to report on the potential health impact of particulate pollution. It is hypothesized that smaller particles can penetrate deeper in lungs and have larger surface area to react within lungs, and the toxicity of particles increases as the particle size decreases [36].

Many of the techniques used to mitigate particulate mass (PM) cause of increase in PN, this increase is primarily in the nucleation mode. Apart from the PM limit, which is already part of the current emissions standard regulations [65], PN emissions have become regulated for emissions certification tests in many countries. For example, China’s CN5 regulation included

313 the limit of $6x10^{11}$ (#/km) for PN emissions, the EU Commission added a limit of $6x10^{11}$ (#/km)
314 for PN emissions to the Euro 5b regulation for the type approval of diesel light-duty vehicles
315 in 2011 and to Euro 6 regulation for the type approval of gasoline direct injection light-duty
316 vehicles in 2014 [65]. PN emission has become more dominant in the most recent emissions
317 regulation such as WLTP. For example, in real driving emission (RDE) type approval tests for
318 compression ignition vehicles, which is a part of WLTP implemented from Sep 2017, only PN
319 needs to be measured and not PM [65]. This could be owing to the fact that after-treatment
320 systems, such as the diesel particulate filter (DPF) can significantly reduce PM , but it is not
321 very effective at reducing the small particles which are very light with no considerable mass
322 (but are significantly more toxic than their larger counterparts). However, there has been a
323 number of research conducted to improve DPFs recently, such as optimisation of microwave
324 energy consumption in the heating process of composite regeneration [66] or performance
325 enhancement of microwave assisted regeneration in a wall-flow diesel particulate filter or
326 diesel soot continuous regeneration performance based on field synergy theory and model [67-
327 69].

328 In the current method of PM measurement in the recent regulation (Euro 6), which is called
329 PMP (Particle Measuring Program), only solid particles with a size of 23 nm and above are
330 measured [37]. However, sub-23 nm particles are more toxic compared to bigger particles;
331 therefore, this study has a special focus on smaller particles (sub-23 nm).

332 PN emissions are influenced by a number of different factors which may cancel or reinforce
333 the effect of one another under different conditions. The following analysis will first look at
334 the effect of cold start and then the effect of fuel on PN emissions during the custom test.

335 This study used an SMPS particle analyser to sample the exhaust emissions. Each sample took
336 2 min, hence the first and second samples (Stage #1 and #2) are from engine start until the

engine coolant temperature (shown in Figure 2) reaches to ~65 degC, the next three samples (Stage #3, #4 and #5) correspond to the duration in which engine coolant temperature is above ~70 degC (shown in Figure 2) but less than its optimum value, therefore these stages cannot be considered as cold start as per the regulation and also not as steady-state owing to the fact that the engine temperature is still increasing. The data of these stages are of importance as it can show that these sections (which are not cold start) are different to steady-state results. The last two samples (Stage #6 and #7) correspond to steady-state condition as the engine coolant temperature is stable, and therefore can be considered steady state. The findings will be discussed in detail first from the cold start effect point of view and then from the fuel properties.

3.1.1 Cold start effect

Figure 3 shows the PN concentration for all of the tested fuels through the custom test measured by an SMPS. In general, the figure shows that PN increases as the engine warms up, which means that the cold start section has lower PN compared to hot start. As explained, there are 7 consecutive stages (each corresponds to the average of two minutes) from the beginning of the cold start test; and PN emissions during each stage will be discussed.

Stages #1 and # 2 fall in the cold start period. As per the regulation, cold start is defined from the engine start (after a proper soak) until 5 minutes or until the engine coolant temperature reaches 70 degC. As can be seen, Stages #1 and #2 had a similar PN concentration for all the fuels. For example, with D100, PN concentration from Stages #1 and #2 were 1.50E7 and 1.52E7; and the difference was less than 1.5%. With D95W5 the difference between Stages #1 and 2 was less than ~1.7%. These two stages correspond to the first 300 s of the test where the engine coolant temperature (shown in Figure 2) increased from ~23 to ~65 degC. During these two stages the engine injection strategy did not change. This can be seen by analysing the start of injection parameter which is a part of injection strategy commanded by the engine controlling unit (shown in Figure 4). As can be seen in Figure 4, during this period, the start of

injection was constant which could be one of the reasons for the insignificant change in PN concentration during this period.

Stage #3 has a significantly higher PN when compared to cold start (Stages #1 and #2). For example, in Stage #3, D100, D99W1 and D95W5 had 32, 74 and 70% higher PN compared to Stage #1. This stage cannot be considered as cold start according to the regulation as it corresponds to a time that the engine coolant temperature has already reached 65 degC (shown in Figure 2) and the injection strategy is changing. This stage is related to an unsteady warm condition. Figure 4 shows a slight change in the start of injection in Stage #3 when compared to Stages #1 and #2. However, Figure 4 cannot show a significant change owing to the fact that it shows the average value over 2 minutes. But, inspecting further showed that during this stage, the start of injection increased (commanded by engine injection strategy) providing the reason for the unsteady condition during this stage.

Stages #4 and #5 are not cold start as per the regulation because the coolant temperature shown in Figure 2 is above 70 degC. However, this duration cannot represent the steady state condition; as the engine exhaust gas, oil and coolant temperatures are still increasing (Figure 2). As shown in Figure 4, in this period, the start of injection is stable; however, it changed compared to Stage #1 and #2 because of the increase in engine temperature. As shown in Figure 3, PN for Stages #4 and #5 are higher than cold start (Stages #1 and #2) for all of the fuels. For example, Stage 4 shows that D100 with 2.34E7 has 56% higher PN than Stage #1 and also 56% than Stage #2.

Stages #6 and #7 represent the hot start steady state condition as they were collected in a duration in which the engine coolant temperature was above 70 degC and also optimal, as shown in Figure 2. These two stages represent the steady-state condition owing to the engine being stable as the start of injection (Figure 4); and coolant, oil and exhaust gas temperatures

386 (Figure 2) are stable. As can be seen in Figure 3, PN concentration for all the fuels are higher
387 during these steady state stages when compared to during cold start. PN with D100, D99W1
388 and D95W5 during steady state (Stage #7) is 54%, 46% and 197% higher than cold start (Stage
389 #1), respectively.

390

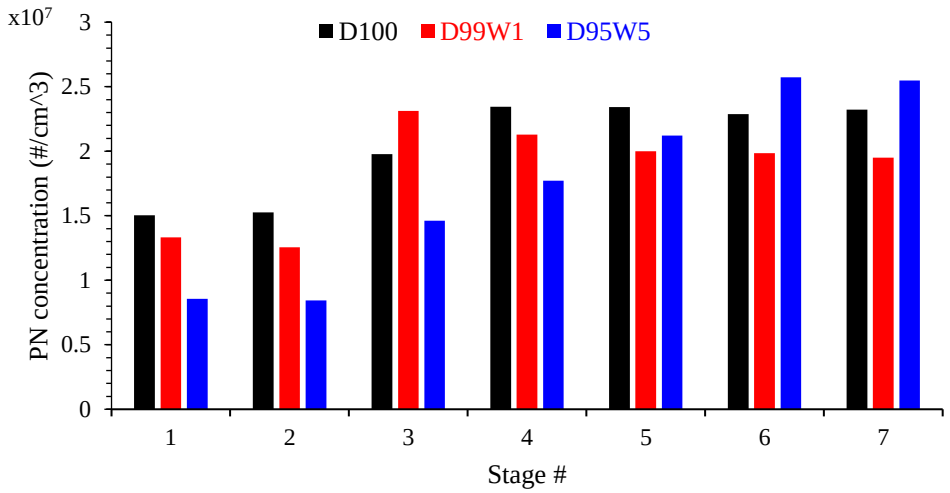

391

392 Figure 3 PN concentration within the custom test for all the tested fuels

393

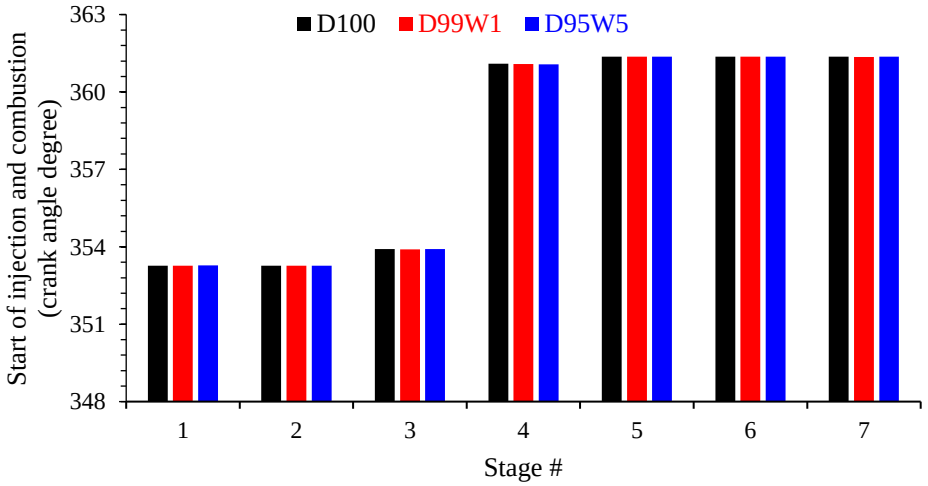

394

395 Figure 4 Start of injection within the custom test

396

Nanoparticles are the main contributor of PN emissions. A study in the literature reported that nanoparticles increase as the exhaust gas temperature increases [35]. Figure 5, which shows the size distribution of the particles for all the tested fuels through the custom test, indicates that the number of nucleation mode particles increases as the engine warms up. To better understand the effect of temperature on PN, this study looks at the size of particles in each stage.

Based on the size distribution, particles can fall into two main categories: nucleation mode and accumulation mode. Nucleation mode particles have a diameter of 3-30 nm. The particles in this mode consist of sulfur, volatile organic compounds and also small portion of solid compounds from carbon and metal [70]. These small particles which are significantly affected by dilution parameters and sampling systems typically contribute 0.1 to 10% of PM and up to 90% of PN [70]. The other category is the accumulation mode, which covers particles with a diameter of 30-500 nm. Adsorbed materials and carbonaceous agglomerates compose the particles in this mode [70]. Condensation of volatile materials which can lead to the agglomeration of particles in the nucleation mode can form accumulation mode particles [71].

As mentioned, PN in **Stages #1 and #2** were similar, shown in Figure 3. Having a similar trend for all of the fuels may conclude that during this period increasing the engine temperature did not affect the PN concentration. As can be seen in Figure 5, separately for each fuel, the PN size distribution of Stage #1 seems similar to Stage #2; however, looking in detail shows that particles are slightly bigger in Stage #2 than Stage #1. This can be better presented by evaluating the median diameter of the particle size from the size distribution graph (there are other ways of looking into this such as analysing the primary particle size [72]). Figure 6 shows the median diameter in the PN size distribution graph within the custom test for all of the tested fuels. As shown, the median diameter increment from Stage #1 to Stage #2 for D100, D99W1 and D95W5 are 82.8 to 90 nm, 78.7 to 83.5 nm and 82.1 to 82.2 nm, respectively. Given that

the start of injection remained constant, increasing engine temperature through these two stages could be the reason for that.

Comparing Stage #2 to **Stage #3** in Figure 6 shows that the median diameter for D100 and D99W1 increased from 90 and 83.5 nm (in Stage #2) to 99 nm and 97 nm (in Stage #3), respectively. While, for D95W5 the median diameter did not change significantly; it slightly decreased from 82.2 to 80.9 nm. Figure 4 shows that for Stage #3, compared to Stages #1 and #2, the start of injection slightly increased as within Stage #3, the injection strategy of the engine changes the start of injection, and given that Figure 4 shows the average value over 2 minutes, the conclusion about the correlation between injection parameters and particle size might not be very accurate.

Figure 6 shows that with D100 and D99W1, **Stage #4** has bigger particles than cold start (Stages #1 and #2), while, D95W5 has smaller particles. Figure 6 also shows that **Stages #4 and #5** have smaller particles compared to Stage #3. The figure also shows that the median diameter after Stage #3 started decreasing; this can be owing to the increasing number of particles in the nucleation mode shown in Figure 5. This increase is more significant when it comes to D95W5, which has more waste lubricating oil in it. This is because of the fuel properties which will be discussed further in the fuel effect sub-section, Section 3.1.2. Looking at Figure 4 and further analysis of the injection parameters showed that the ignition delay during these two stages are higher than Stage #3, consequently there will be more time for fuel atomisation and evaporation.

With D100 and D95W5, **Stages #6 and #7** have smaller particles compared to cold start and also other stages. With D95W5, the nucleation mode particles increase gradually as the engine warms up, this could be the reason for the higher PN emissions as nucleation mode particles are the main contributor. Figure 4 and further analysis of the injection parameters showed that

446 the ignition delay during these two steady state stages are higher than cold start stages,
447 therefore, there will be better fuel atomisation during these stages which can be another reasons
448 for smaller particles. However, despite this, the driving force for this increase is likely to be
449 the fuel properties.

450

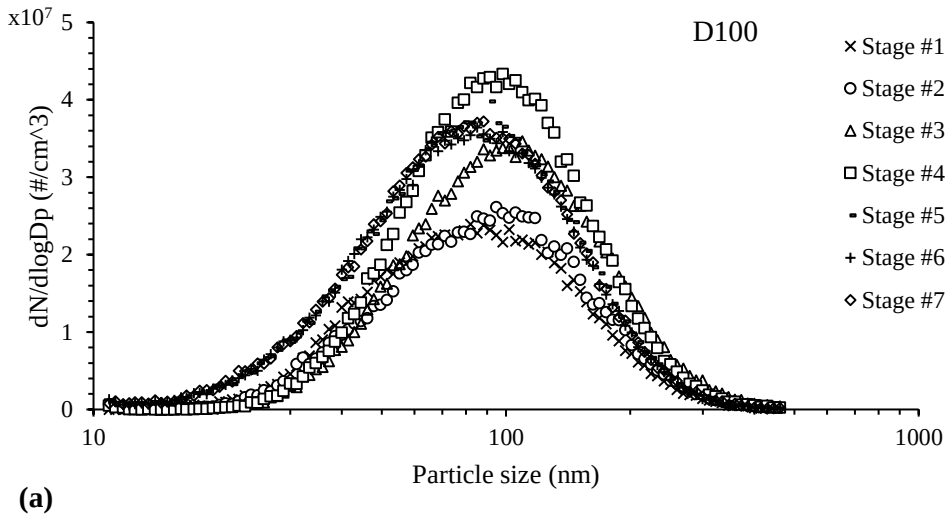

(a)

451

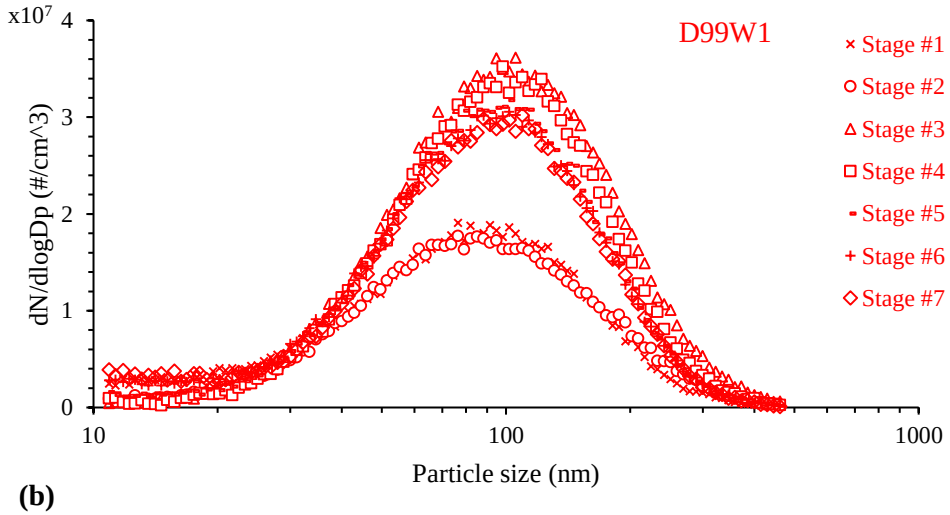

(b)

452

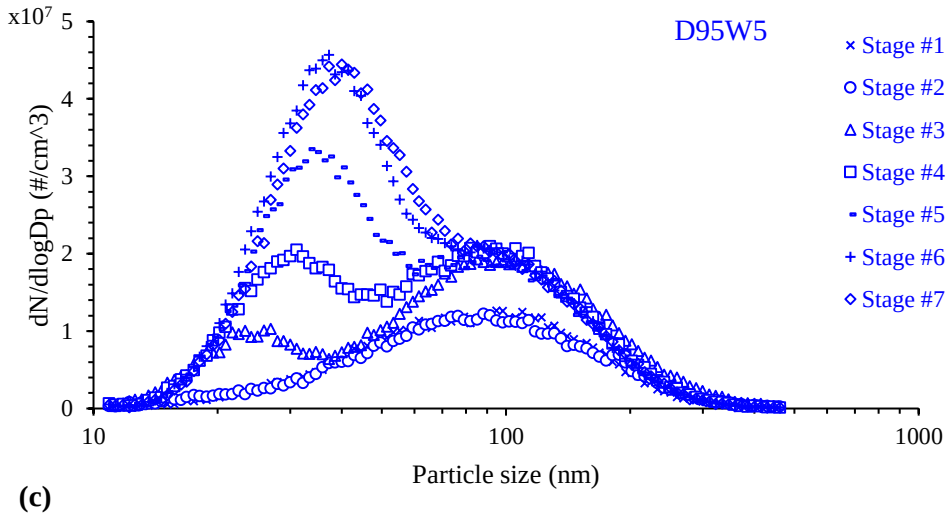

(c)

453

454 Figure 5 PN size distribution within the custom test for all the tested fuels

455

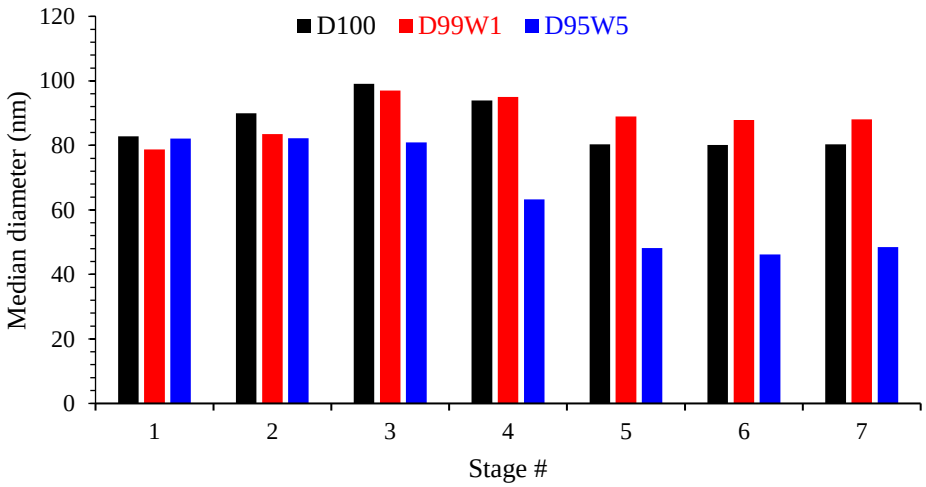

Figure 6 Median diameter in PN size distribution within the custom test for all the tested fuels

3.1.2 Fuel effect

In terms of the fuel effect, Figure 3 shows that D95W5 has the highest PN when the engine is fully warmed up; while, during cold start it has the lowest PN and D100 has the highest value. With D95W5, as the engine was warming up, the PN size distribution moved toward a bimodal distribution with an increasing nucleation mode particle domination due to the presence of waste lubricating oil. It is shown in the literature that the sulfur content of fuel or lubricating oil can cause a significant increase in nucleation mode particles which have a size of less than 30 nm [35, 73, 74].

Stages #1 and #2 indicate that during cold start D100 has the highest PN and increasing the share of waste lubricating oil decreases PN emissions, as shown in Figure 3. For example, during Stage #1, PN was 1.5E7 with D100 and adding 1 and 5% waste lubricating oil decreased PN by 11 and 43%, respectively. Similarly, for Stage #2, the decrease was 18 and 45%, respectively. In terms of the fuel effect on size distribution, Stages #1 and 2 in Figures 5 and 6 show that adding waste lubricating oil to the blend decreases the size of the particles. This

weakens the effect of temperature rise on the size of particles. This can be seen from the median diameter change from Stage #1 to Stage #2, where the start of injection (shown in Figure 4) was constant and the increase in the engine temperature—which itself was associated with an increase in median diameter for each fuel—will be less effective when the share of waste lubricating oil in the fuel increases. For example, for D100, the increase from Stage #1 to Stage #2 was ~7 nm while for D99W1 and D95W5 the increase were ~4 nm and 0 nm, respectively.

During **Stage #3**, D95W5 has the lowest PN, similar to Stages #1 and #2; however, the difference between PN with D95W5 and the fuel with the highest PN decreased through these three stages. **During Stage #4**, D95W5 has the lowest PN, similar to Stages #1, #2 and #3; however, the difference between PN with D95W5 and the fuel with the highest PN decreased through these four stages and eventually PN with D95W5 from **Stage #5** onward was not the lowest value compared to the other fuel. This is because of the increasing trend of nucleation mode particles (shown in Figure 5) owing to the presence of waste lubricating oil, which significantly affects the PN emissions.

Figure 3 shows that in **Stages #6 and #7**, D95W5 has the highest PN between the fuels. For example, in Stage #6, D95W5 has 2.6E7 PN which is ~13% higher than D100. The reason can be better explained by looking at the size of the particles. Smaller particles typically have a greater contribution to the total PN and particles with bigger median diameter contributes more to larger particles [75]. Figure 6 shows that the median diameter of particles with D95W5 in Stages #6 and 7 is less than 50 nm while for the other two fuels it is above 80 nm. This significantly lowers the median diameter compared to the other two fuels and explains the higher PN. Figure 5 shows that with D95W5, from Stage #1 to Stage #7 the number of particles in the nucleation mode increases, making a more visible bimodal size distribution. An increase in the nucleation mode particles decreases the median diameter as shown in Figure 6. This is owing to the presence of 5% waste lubricating oil in the fuel, which increases the nucleation

mode particles consequently decreasing the median diameter. As mentioned before, PN and PN size distribution are affected by different parameters cancelling or reinforcing the effect of one another under different condition.

A study by Kittelson et al. [35] showed that the sulfur content of lubricating oil increased the nanoparticles. Nucleation mode particles—which mainly form during the exhaust gas cooling and dilution process—are composed of soluble and volatile organic fractions formed from the portion of fuel and evaporated lubricating oil which escaped from the oxidation process [76]. Therefore, higher evaporated lubricating oil can potentially increase the nucleation mode particles. During cold start, the low temperature of the cylinder wall leads to a lower temperature of the charged air in the cylinder. This, and also the low temperature of the fuel, will negatively impact the fuel and lubricating oil vaporization, leading to less nucleation mode particles during cold start; however, by increasing the engine temperature the charged air temperature in cylinder increases, leading to better fuel vaporization and increased evaporated lubricating oil which consequently increases nucleation mode particles. Given that the presence of lubricating oil during combustion affects the nucleation mode particles, compared to D100 the fuel blends with waste lubricating oil (D99W1 and D95W5) have more nucleation mode particles as the engine warms up. This can be seen in Figure 5 where the nucleation mode particles with D95W5 increases significantly as the engine warms up.

3.2 Friction losses and mechanical efficiency

FMEP is the difference between indicated mean effective pressure (IMEP) and brake mean effective pressure (BMEP). This parameter indicates the engine friction losses from different parts of the engine, such as pumps (fuel, water and oil pumps) and mechanical friction. Figure 7 shows the FMEP within the custom test through 7 stages, each corresponds to the average of

two minutes from the beginning of the cold start test. As can be seen, FMEP during cold start is higher than during the hot section. For example, with D100, FMEP from Stage #1 which is related to the first two minutes of the test is 146% higher compared to Stage #7 in when the engine is warmed up. As can be seen from Figure 7, FMEP decreases as the engine warms up. For example, compared to Stage #1, the FMEP reduction with D100 in Stage #2 to #7 was 24.6, 35.7, 46.3, 53.6, 56.6, and 59.4%, respectively. Or with D95W5, the decrease compared to Stage #1 was 20.6, 33.7, 46.4, 53.6, 54.3 and 57.7% for Stage #2 to #7, respectively. The reason for the higher FMEP during cold start is due to the higher viscosity of the lubricating oil because of its low temperature. As the engine warms up, the engine oil temperature increases and consequently the lubricant viscosity decreases which leads to less friction losses, therefore less FMEP. Comparing Figure 2 to Figure 7 shows the correlation between FMEP and engine oil temperature. As can be seen from Stage #1 to Stage #4, the FMEP decrease was significant corresponding to a significant increase in engine oil temperature through these stages; while, from Stage #4 to Stage #7 the FMEP decreased gradually with a lower rate, similar to the lower lubricating oil temperature rise rate when compared to the rate from Stages #1 to #4.

FMEP is affected by other parameters as well. As can be seen in Figure 7, by adding waste lubricating oil to the fuel FMEP increases. For example, in Stage #7, FMEP with D100 is 69.5 kPa, but adding 1 and 5% waste lubricating oil increased FMEP to 69.7 and 73.7 kPa, or in Stage #3 in which FMEP with D100, D99W1 and D95W5 was 110, 112 and 116 kPa, respectively. It can be also be seen that difference between D95W5 (with 5% waste lubricating oil) and D100 on FMEP is more significant during cold start, compared to when the engine is fully warmed up. For example, in Stages #1 and #2, FMEP with D95W5 is ~8% higher than with D100, while in Stage #7 the difference in 6%. The reason could be due to the lower

viscosity of the waste lubricating oil when the engine is fully warmed up compared to cold start.

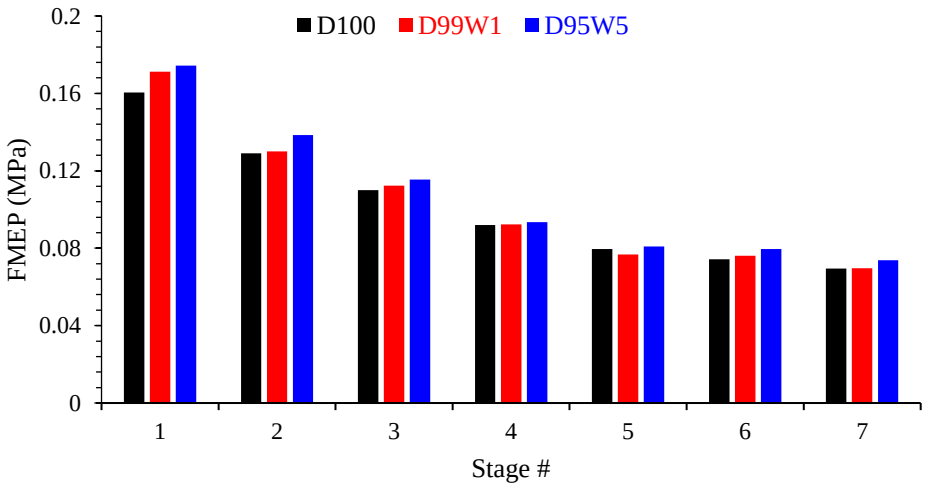

Figure 7 FMEP within the custom test for all the tested fuels

Mechanical efficiency is another parameter which can indicate friction loss in an engine. As can be seen in Figure 8, the mechanical efficiency during cold start is lower than during hot start. For example, in Stage #1, the mechanical efficiency with all of the tested fuels was between 72 to 74%, while in Stage #7, it was ~88%. This parameter also strongly depends on engine oil temperature. As can be seen in Figure 8, the mechanical efficiency increases as the engine warms up. This is because an engine oil temperature increase leads to lower viscosity, less friction, and consequently to less difference between the indicated power and brake power, which increases the mechanical efficiency. Similar to FMEP, this parameter has a strong correlation with engine oil temperature. As can be seen, the increase from Stage #1 to #4 is higher when compared to the increase from Stage #4 to #7, similar to the engine oil temperature increase rate during these two periods. For example, with D100, the mechanical efficiency increased from 73% in Stage #1 to 84% in Stage #4, while in Stage #7, the mechanical

efficiency was 88%. Regarding the effect of fuel on mechanical efficiency, it can be seen from the figure that the difference is not significant, however, in most of the stages D95W5 with 5% waste lubricating oil in the blend had a slightly lower efficiency (nearly 1%) compared to D100 and the other fuel. This aligns with FMEP, as these two parameters have an inverse correlation.

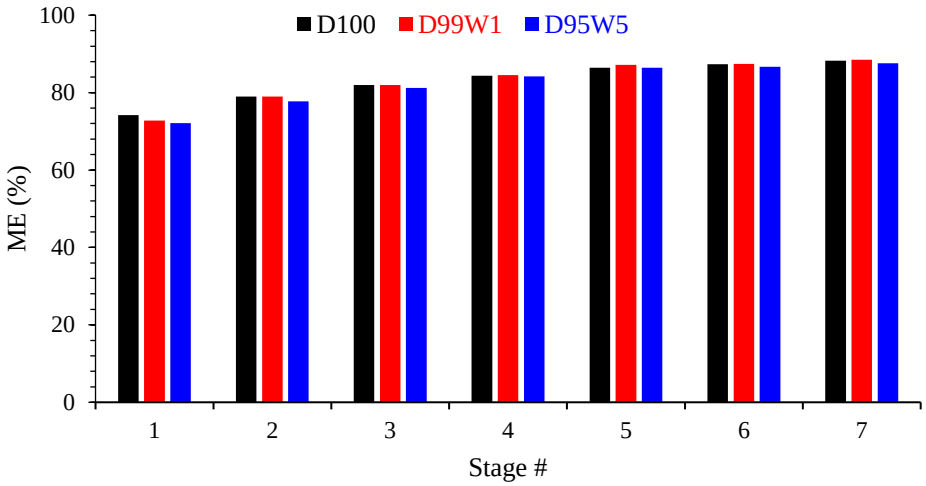

Figure 8 Mechanical efficiency within the custom test for all the tested fuels

3.3 Cyclic variability

Cyclic variability in combustion can have a negative impact on exhaust emissions and engine performance parameters [77]. The reasons behind this instability could be due to different factors such as fuel properties, fuel injection timing and pressure, air/fuel mixture in premixed combustion phase, air-to-fuel ratio, in-cylinder mixture motion, engine operating condition and engine temperature [20, 77, 78]. There are different ways of presenting the combustion instability [79, 80]. This study uses engine speed and indicated mean effective pressure to study the combustion instability.

Given that the cold start test was at constant speed, the first study will be on engine speed by calculating the CoV—standard deviation divided by average—over 2 min stage (which will be ~1440 engine cycles) during the custom test for all the tested fuels. In terms of engine speed stability during the test, the CoV for engine speed was calculated for 7 stages (each two minutes) from the start of the cold start test until the engine was warmed up for all of the tested fuels, shown in Figure 9. As can be seen, the CoV for all of the tested fuels during the test was less than 0.2% which shows the stability of the engine speed during the test. D99W1 had the highest CoV in all of the stages; while, D95W5 had the lowest CoV (except for Stage #1 in which D95W5 was slightly higher than D100). The figure also shows that CoV with D95W5 was slightly higher during cold start (the first three stages) compared to when the engine was warmed up (Stages #6 and #7). As mentioned, the changes are insignificant (less than 0.2%) and the difference seen in the figure might not be meaningful in terms of cold start or fuel effects.

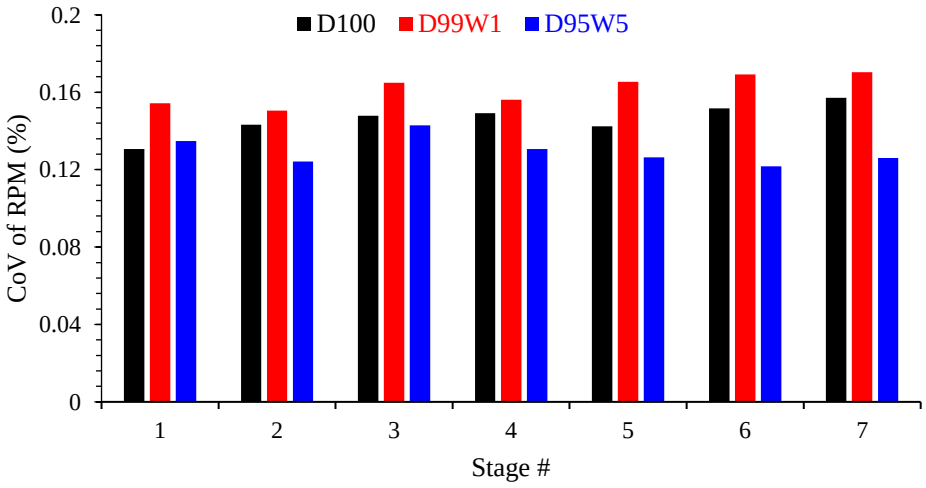

Figure 9 Engine speed coefficient of variation within the custom test for all the tested fuels

598 Figure 10 shows the CoV of IMEP within the custom test for all the tested fuels. As can be
599 seen, the CoV of IMEP during cold start (Stage #1) is significantly higher when compared to
600 Stage #7 in which the engine is warmed up. For example, in Stage #1, the CoV of IMEP with
601 D100, D99W1 and D95W5 are 1.7, 1.2, and 1.1%, respectively; while, in Stage #7 are 0.9, 0.6
602 and 0.6%. Also, it can be seen that this parameter has a decreasing trend as the engine warms
603 up through Stages #1 to #7. The reason for the higher CoV of IMEP during cold start could be
604 the low temperature of the cylinder wall during cold start, which can adversely influence the
605 fuel vaporisation and fuel ignition making the in-cylinder pressure gradient steeper. This can
606 be seen in Figure 11 where the maximum rate of pressure rise is significantly higher during
607 cold start and decreases with increasing engine temperature. For example, with D100, the
608 maximum rate of pressure rise during cold start (Stage #1) is 1.7 times higher than when the
609 engine is warmed up (Stage #7). Generally, noise and instability in diesel engines highly
610 depend on the premixed combustion phase [81], and maximum rate of pressure rise highly
611 depends on the premixed combustion phase.

612

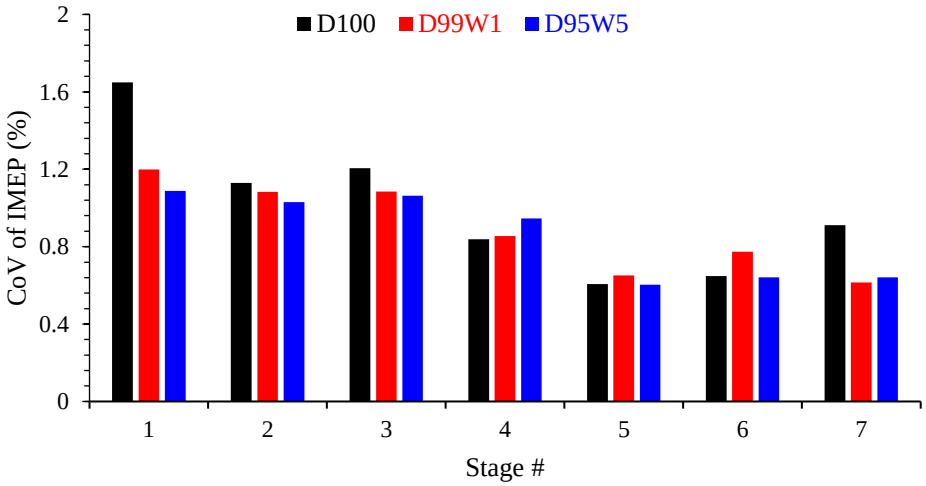

613

614 Figure 10 Coefficient of variation of IMEP within the custom test for all the tested fuels

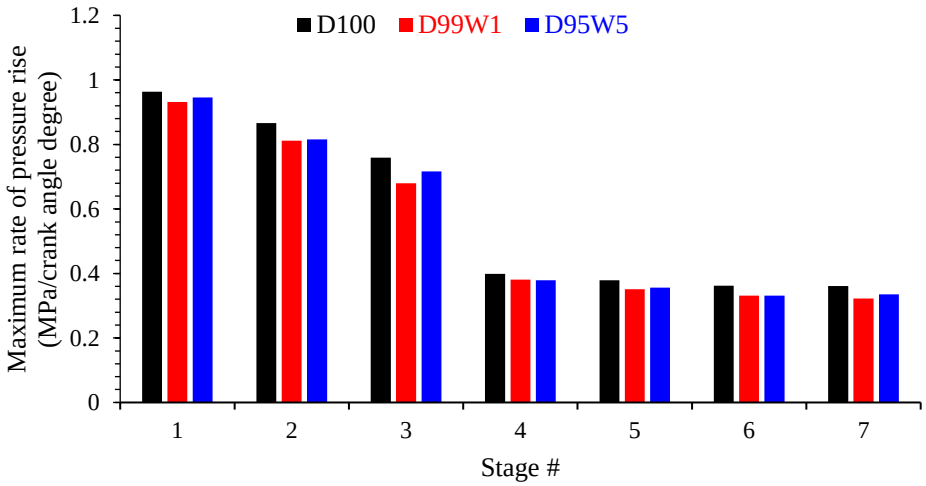

615

616 Figure 11 Maximum rate of pressure rise within the custom test for all the tested fuels

617

618 **4. Conclusions**

619 This study investigated the particulate matter emissions and engine performance parameters
620 within cold start and hot engine operation using a custom cold start test running on a 6-cylinder
621 turbocharged diesel engine. It also studied the influence of lubricating oil on the combustion
622 process as well as evaluating the possibility of using waste lubricating oil as a fuel by using
623 two blends of diesel with 1 and 5% waste lubricating oil. The parameters studied in this
624 research were PN, friction losses and combustion instability. In this study, in order to better
625 explain the observed trends, other parameters such as engine oil, coolant and exhaust gas
626 temperatures; start of injection; FMEP; mechanical efficiency; CoV of engine speed; CoV of
627 IMEP; and maximum rate of pressure rise were studied. Following conclusions were drawn:

628 • During the first two stages of cold start, PN concentration did not change considerably
629 owing to the fixed injection strategy.

- During Stage #3, which was after the cold start threshold (defined by the engine strategy), PN increased up to 74% due to the injection strategy change and unstable condition.
- Stages #4 and #5, which are not cold start and also not steady state, had a similar PN but higher than cold start stages.
- Stage #7, which was related to the steady state condition, had 54% higher PN than cold start when diesel was used. With 5% waste lubricating oil in the fuel blend, this PN increase was 197%.
- Nucleation mode particles increased as the engine warmed up. During cold start, an increase in engine temperature was associated with an increase in particle size, while during hot operation and steady state, an increase in engine temeprature was associated with a decrease in particle size. This was owing to an increase in nucleation mode particles.
- During cold start, adding 5% waste lubricating oil to the blend decreased PN by 43%, while during steady state it increased PN by ~13%.
- Adding waste lubricating oil significantly increased the number of nucleation mode particles and decreased the size of the particles during steady state.
- Compared to steady state, during cold start FMEP was higher (~146%) and mechanical efficiency was lower (~15%).
- Adding waste lubricating oil to the fuel increased the FMEP and slightly decreased the mechanical efficiency.
- The CoV of IMEP and maximum rate of pressure rise during cold start were higher than steady state. Adding waste lubricating oil to the fuel during cold start decreased the CoV of IMEP and the maximum rate of pressure rise.

5. Acknowledgement

This research was supported by the Australian Research Council Linkage Projects funding scheme (project number LP110200158). Authors would like to acknowledge Prof. Jochen Mueller, Mr. Andrew Elder the software developer from DynoLog Dynamometer Pty Ltd and Mr. Noel Hartnett for their assistance.

6. References

[1] K. Nanthagopal, R. S. Kishna, A. E. Atabani, A. a. H. Al-Muhtaseb, G. Kumar, and B. Ashok, "A compressive review on the effects of alcohols and nanoparticles as an oxygenated enhancer in compression ignition engine," *Energy Conversion and Management,* vol. 203, p. 112244, 2020/01/01/ 2020.

[2] U. Rajak and T. N. Verma, "A comparative analysis of engine characteristics from various biodiesels: Numerical study," *Energy Conversion and Management,* vol. 180, pp. 904-923, 2019/01/15/ 2019.

[3] J. M. Fonseca, J. G. Teleken, V. de Cinque Almeida, and C. da Silva, "Biodiesel from waste frying oils: Methods of production and purification," *Energy Conversion and Management,* vol. 184, pp. 205-218, 2019/03/15/ 2019.

[4] M. Aghbashlo, M. Tabatabaei, P. Mohammadi, B. Khoshnevisan, M. A. Rajaeifar, and M. Pakzad, "Neat diesel beats waste-oriented biodiesel from the exergoeconomic and exergoenvironmental point of views," *Energy Conversion and Management,* vol. 148, pp. 1-15, 2017/09/15/ 2017.

[5] O. Tóth, A. Holló, and J. Hancsók, "Co-processing a waste fatty acid mixture and unrefined gas oil to produce renewable diesel fuel-blending components," *Energy Conversion and Management,* vol. 185, pp. 304-312, 2019/04/01/ 2019.

[6] S. Shafiee and E. J. E. p. Topal, "When will fossil fuel reserves be diminished?," vol. 37, no. 1, pp. 181-189, 2009.

[7] J. E *et al.*, "Effect of different technologies on combustion and emissions of the diesel engine fueled with biodiesel: A review," *Renewable and Sustainable Energy Reviews,* vol. 80, pp. 620-647, 2017/12/01/ 2017.

[8] S. Amid *et al.*, "Effects of waste-derived ethylene glycol diacetate as a novel oxygenated additive on performance and emission characteristics of a diesel engine fueled with diesel/biodiesel blends," *Energy Conversion and Management,* vol. 203, p. 112245, 2020/01/01/ 2020.

[9] P. Verma *et al.*, "Diesel engine performance and emissions with fuels derived from waste tyres," *Scientific reports,* vol. 8, no. 1, p. 2457, 2018.

[10] M. N. Nabi, A. Zare, F. M. Hossain, Z. D. Ristovski, and R. J. J. J. o. c. p. Brown, "Reductions in diesel emissions including PM and PN emissions with diesel-biodiesel blends," vol. 166, pp. 860-868, 2017.

[11] A. Zare *et al.*, "The effect of triacetin as a fuel additive to waste cooking biodiesel on engine performance and exhaust emissions," *Fuel,* vol. 182, pp. 640-649, 2016.

[12] A. Zare *et al.*, "The influence of oxygenated fuels on transient and steady-state engine emissions," *Energy*, vol. 121, pp. 841-853, 2017.
[13] A. Zare, T. A. Bodisco, M. N. Nabi, F. M. Hossain, Z. D. Ristovski, and R. J. J. E. Brown, "Engine performance during transient and steady-state operation with oxygenated fuels," *Energy and fuels*, vol. 31, no. 7, pp. 7510-7522, 2017.
[14] A. Zare *et al.*, "Impact of Triacetin as an oxygenated fuel additive to waste cooking biodiesel: transient engine performance and exhaust emissions," in *Proceedings of the 2015 Australian Combustion Symposium*, 2015, pp. 48-51: The Combustion Institute Australia and New Zealand Section.
[15] M. N. Nabi, A. Zare, F. M. Hossain, T. A. Bodisco, Z. D. Ristovski, and R. J. Brown, "A parametric study on engine performance and emissions with neat diesel and diesel-butanol blends in the 13-Mode European Stationary Cycle," *Energy conversion and management*, vol. 148, pp. 251-259, 2017.
[16] M. Fuentes, R. Font, M. Gómez-Rico, I. J. J. o. A. Martín-Gullón, and A. Pyrolysis, "Pyrolysis and combustion of waste lubricant oil from diesel cars: Decomposition and pollutants," vol. 79, no. 1-2, pp. 215-226, 2007.
[17] M. André, "In actual use car testing: 70,000 kilometers and 10,000 trips by 55 French cars under real conditions," *SAE transactions*, pp. 65-72, 1991.
[18] M. S. Reiter, K. M. J. T. R. P. D. T. Kockelman, and Environment, "The problem of cold starts: a closer look at mobile source emissions levels," vol. 43, pp. 123-132, 2016.
[19] J.-M. André and R. Joumard, "Modelling of cold start excess emissions for passenger cars," 2005.
[20] A. Zare, T. A. Bodisco, M. N. Nabi, F. M. Hossain, Z. D. Ristovski, and R. J. Brown, "A comparative investigation into cold-start and hot-start operation of diesel engine performance with oxygenated fuels during transient and steady-state operation," *Fuel*, vol. 228, pp. 390-404, 2018/09/15/ 2018.
[21] A. Zare *et al.*, "Diesel engine emissions with oxygenated fuels: A comparative study into cold-start and hot-start operation," *Journal of cleaner production*, vol. 162, pp. 997-1008, 2017.
[22] A. Roberts, R. Brooks, P. J. E. C. Shipway, and Management, "Internal combustion engine cold-start efficiency: A review of the problem, causes and potential solutions," vol. 82, pp. 327-350, 2014.
[23] Y. Cao, "Operation and cold start mechanisms of internal combustion engines with alternative fuels," SAE Technical Paper0148-7191, 2007.
[24] E. G. Giakoumis, C. D. Rakopoulos, A. M. Dimaratos, D. C. J. P. i. E. Rakopoulos, and C. Science, "Exhaust emissions of diesel engines operating under transient conditions with biodiesel fuel blends," vol. 38, no. 5, pp. 691-715, 2012.
[25] R. A. Sakunthalai, H. Xu, D. Liu, J. Tian, M. Wyszynski, and J. Piaszyk, "Impact of cold ambient conditions on cold start and idle emissions from diesel engines," SAE Technical Paper0148-7191, 2014.
[26] E. Nam, *Analysis of particulate matter emissions from light-duty gasoline vehicles in Kansas City*. US Environmental Protection Agency, 2008.
[27] P. Bielaczyc, J. Merkisz, and J. Pielecha, "A method of reducing the exhaust emissions from DI diesel engines by the introduction of a fuel cut off system during cold start," SAE Technical Paper0148-7191, 2001.
[28] D.-W. Lee, J. Johnson, J. Lv, K. Novak, and J. Zietsman, "Comparisons between vehicular emissions from real-world in-use testing and EPA moves estimation," Texas Transportation Institute2012.

[29] J. E *et al.*, "Effect analysis on cold starting performance enhancement of a diesel engine fueled with biodiesel fuel based on an improved thermodynamic model," *Applied Energy*, vol. 243, pp. 321-335, 2019/06/01/ 2019.
[30] Y. Deng, H. Liu, X. Zhao, J. E, and J. Chen, "Effects of cold start control strategy on cold start performance of the diesel engine based on a comprehensive preheat diesel engine model," *Applied Energy*, vol. 210, pp. 279-287, 2018/01/15/ 2018.
[31] B. J. Mitchell *et al.*, "Engine blow-by with oxygenated fuels: A comparative study into cold and hot start operation," *Energy*, vol. 140, pp. 612-624, 2017.
[32] F. Will and A. Boretti, "A new method to warm up lubricating oil to improve the fuel efficiency during cold start," *SAE international journal of engines*, vol. 4, no. 1, pp. 175-187, 2011.
[33] C. Samhaber, A. Wimmer, and E. Loibner, "Modeling of engine warm-up with integration of vehicle and engine cycle simulation," SAE Technical Paper0148-7191, 2001.
[34] T. Chu Van *et al.*, "Effect of cold start on engine performance and emissions from diesel engines using IMO-Compliant distillate fuels," *Environmental Pollution*, vol. 255, p. 113260, 2019/12/01/ 2019.
[35] D. Kittelson *et al.*, "Effect of fuel and lube oil sulfur on the performance of a diesel exhaust gas continuously regenerating trap," vol. 42, no. 24, pp. 9276-9282, 2008.
[36] J. Krahl, J. Bünger, O. Schröder, A. Munack, and G. J. J. o. t. A. O. C. S. Knothe, "Exhaust emissions and health effects of particulate matter from agricultural tractors operating on rapeseed oil methyl ester," vol. 79, no. 7, pp. 717-724, 2002.
[37] G. Martini, B. Giechaskiel, and P. J. B. Dilara, "Future European emission standards for vehicles: the importance of the UN-ECE Particle Measurement Programme," vol. 14, no. sup1, pp. 29-33, 2009.
[38] B. Giechaskiel, T. Lähde, and Y. Drossinos, "Regulating particle number measurements from the tailpipe of light-duty vehicles: The next step?," *Environmental Research*, vol. 172, pp. 1-9, 2019/05/01/ 2019.
[39] Z. Uriondo, G. Gabiña, O. C. Basurko, M. Clemente, S. Aldekoa, and L. J. F. Martin, "Waste lube-oil based fuel characterization in real conditions. Case study: Bottom-trawl fishing vessel powered with medium speed diesel engine," vol. 215, pp. 744-755, 2018.
[40] T. Bhaskar *et al.*, "Recycling of waste lubricant oil into chemical feedstock or fuel oil over supported iron oxide catalysts," *Fuel*, vol. 83, no. 1, pp. 9-15, 2004/01/01/ 2004.
[41] O. Arpa, R. Yumrutaş, and Z. J. F. p. t. Argunhan, "Experimental investigation of the effects of diesel-like fuel obtained from waste lubrication oil on engine performance and exhaust emission," vol. 91, no. 10, pp. 1241-1249, 2010.
[42] H. Park, J. Shin, and C. Bae, "Spray and Combustion of Diesel Fuel under Simulated Cold-Start Conditions at Various Ambient Temperatures," 2017. Available: https://doi.org/10.4271/2017-24-0069
[43] M. N. Nabi *et al.*, "Influence of fuel-borne oxygen on European Stationary Cycle: Diesel engine performance and emissions with a special emphasis on particulate and NO emissions," *Energy conversion and management*, vol. 127, pp. 187-198, 2016.
[44] T. Bodisco and A. Zare, "Practicalities and Driving Dynamics of a Real Driving Emissions (RDE) Euro 6 Regulation Homologation Test," *Energies*, vol. 12, no. 12, p. 2306, 2019.
[45] N. Nabi *et al.*, "Formulation of new oxygenated fuels and their influence on engine performance and exhaust emissions," in *Proceedings of the 2015 Australian Combustion Symposium*, 2015, pp. 64-67: The Combustion Institute Australia and New Zealand Section.

[46] C. Odibi *et al.*, "Exergy analysis of a diesel engine with waste cooking biodiesel and triacetin," vol. 198, p. 111912, 2019.
[47] T. Chu-Van *et al.*, "On-board measurements of particle and gaseous emissions from a large cargo vessel at different operating conditions," *Environmental Pollution*, vol. 237, pp. 832-841, 2018/06/01/ 2018.
[48] T. Bodisco and R. J. J. E. Brown, "Inter-cycle variability of in-cylinder pressure parameters in an ethanol fumigated common rail diesel engine," vol. 52, pp. 55-65, 2013.
[49] T. Bodisco, P. Tröndle, and R. J. J. E. Brown, "Inter-cycle variability of ignition delay in an ethanol fumigated common rail diesel engine," vol. 84, pp. 186-195, 2015.
[50] H. Li *et al.*, "Study of thermal characteristics and emissions during cold start using an on-board measuring method for modern SI car real world urban driving," vol. 1, no. 1, pp. 804-819, 2009.
[51] A. Roberts, R. Brooks, and P. Shipway, "Internal combustion engine cold-start efficiency: A review of the problem, causes and potential solutions," *Energy Conversion and Management*, vol. 82, pp. 327-350, 2014.
[52] G. E. Andrews, A. M. Ounzain, H. Li, M. Bell, J. Tate, and K. Ropkins, "The Use of a Water/Lube Oil Heat Exchanger and Enhanced Cooling Water Heating to Increase Water and Lube Oil Heating Rates in Passenger Cars for Reduced Fuel Consumption and CO2 Emissions During Cold Start," SAE Technical Paper0148-7191, 2007.
[53] L. Jarrier, J. Champoussin, R. Yu, and D. Gentile, "Warm-up of a DI diesel engine: experiment and modeling," SAE Technical Paper0148-7191, 2000.
[54] J. Trapy and P. Damiral, "An investigation of lubricating system warm-up for the improvement of cold start efficiency and emissions of SI automotive engines," SAE Technical Paper902089, 1990.
[55] H. Li *et al.*, "Study of thermal characteristics and emissions during cold start using an on-board measuring method for modern SI car real world urban driving," *SAE International Journal of Engines*, vol. 1, no. 1, pp. 804-819, 2009.
[56] K. Kunze, S. Wolff, I. Lade, and J. Tonhauser, "A systematic analysis of CO2-reduction by an optimized heat supply during vehicle warm-up," SAE Technical Paper0148-7191, 2006.
[57] P. Verma *et al.*, "An overview of the influence of biodiesel, alcohols, and various oxygenated additives on the particulate matter emissions from diesel engines," *Energies*, vol. 12, no. 10, p. 1987, 2019.
[58] World Health Organization, "Review of Evidence on Health Aspects of Air Pollution—REVIHAAP Project," *WHO Regional Office for Europe: Copenhagen, Denmark*, 2013.
[59] S. Stevanovic *et al.*, "Oxidative potential of gas phase combustion emissions - An underestimated and potentially harmful component of air pollution from combustion processes," *Atmospheric Environment*, vol. 158, pp. 227-235, 2017/06/01/ 2017.
[60] A. Vaughan *et al.*, "N-acetyl cysteine (NAC) intervention attenuates the effects of diesel and biodiesel emission exposure on human bronchial epithelial cells, 16HBE, at air-liquid interface," ed: Eur Respiratory Soc, 2016.
[61] F. Hedayat *et al.*, "Influence of oxygen content of the certain types of biodiesels on particulate oxidative potential," vol. 545, pp. 381-388, 2016.
[62] A. Vaughan *et al.*, "Removal of organic content from diesel exhaust particles alters cellular responses of primary human bronchial epithelial cells cultured at an air-liquid interface," *Journal of Environmental*

Analytical Toxicology, vol. 5, no. 5, pp. 100316-1, 2015.

[63] A. Vaughan *et al.*, "organic Content Of Diesel Emission Particles And Human Bronchial Epithelial Cell Responses To Primary And Aged Diesel Emissions: tp 032," *Respirology*, vol. 20, p. 74, 2015.
[64] A. Vaughan *et al.*, "The cytotoxic, inflammatory and oxidative potential of coconut oil-substituted diesel emissions on bronchial epithelial cells at an air-liquid interface," vol. 26, no. 27, pp. 27783-27791, 2019.
[65] Delphi. (2018, 15/04/2019). *Worldwide emissions standards*. Available: https://www.delphi.com/innovations#emissionstandards
[66] J. E *et al.*, "Effects analysis on optimal microwave energy consumption in the heating process of composite regeneration for the diesel particulate filter," *Applied Energy*, vol. 254, p. 113736, 2019/11/15/ 2019.
[67] E. Jiaqiang *et al.*, "Performance enhancement of microwave assisted regeneration in a wall-flow diesel particulate filter based on field synergy theory," *Energy*, vol. 169, pp. 719-729, 2019/02/15/ 2019.
[68] X. Zhao *et al.*, "A review on heat enhancement in thermal energy conversion and management using Field Synergy Principle," *Applied Energy*, vol. 257, p. 113995, 2020/01/01/ 2020.
[69] J. E *et al.*, "Effects analysis on diesel soot continuous regeneration performance of a rotary microwave-assisted regeneration diesel particulate filter," *Fuel*, vol. 260, p. 116353, 2020/01/15/ 2020.
[70] D. Kittelson, W. Watts, and J. J. F. r. Johnson, Coordinating Research Council, "Diesel Aerosol Sampling Methodology–CRC E-43," 2002.
[71] M. S. Peckham, A. Finch, B. Campbell, P. Price, and M. T. Davies, "Study of particle number emissions from a turbocharged gasoline direct injection (GDI) engine including data from a fast-response particle size spectrometer," SAE Technical Paper0148-7191, 2011.
[72] P. Verma, E. Pickering, N. Savic, A. Zare, R. Brown, and Z. Ristovski, "Comparison of manual and automatic approaches for characterisation of morphology and nanostructure of soot particles," *Journal of Aerosol Science*, vol. 136, pp. 91-105, 2019/10/01/ 2019.
[73] D. B. Kittelson *et al.*, "Driving down on-highway particulate emissions," SAE Technical Paper0148-7191, 2006.
[74] D. Kittelson *et al.*, "On-road evaluation of two diesel exhaust aftertreatment devices," vol. 37, no. 9, pp. 1140-1151, 2006.
[75] M. Jafari *et al.*, "Multivariate analysis of performance and emission parameters in a diesel engine using biodiesel and oxygenated additive," *Energy Conversion and Management*, vol. 201, p. 112183, 2019/12/01/ 2019.
[76] D. B. Kittelson, M. Arnold, and W. F. Watts, *Review of diesel particulate matter sampling methods*. University of Minnesota, Department of Mechanical Engineering, Center for …, 1999.
[77] Y. Wang, F. Xiao, Y. Zhao, D. Li, and X. Lei, "Study on cycle-by-cycle variations in a diesel engine with dimethyl ether as port premixing fuel," *Applied energy*, vol. 143, pp. 58-70, 2015.
[78] J. Bittle, B. Knight, and T. Jacobs, "Biodiesel effects on cycle-to-cycle variability of combustion characteristics in a common-rail medium-duty diesel engine," SAE Technical Paper0148-7191, 2010.
[79] L.-P. Yang, T. A. Bodisco, A. Zare, N. Marwan, T. Chu-Van, and R. J. J. N. D. Brown, "Analysis of the nonlinear dynamics of inter-cycle combustion variations in an ethanol fumigation-diesel dual-fuel engine," pp. 1-20, 2019.

[80] M. Jafari, P. Verma, A. Zare, T. A. Bodisco, Z. Ristovski, and R. J. Brown, "Investigation of diesel engine combustion instability using a dynamical systems approach," in *21st Australasian Fluid Mechanics Conference,* Adelaide, Australia, 2018.
[81] H. Jääskeläinen and M. K. J. E. I. Khair, DieselNet Technology Guide, "Combustion in diesel engines," 2016.

7. Appendix

Test repeatability was ensured by conducting the cold and hot start tests two times. The statistical analysis—average, standard deviation (SD) and coefficient of variation (CoV)—of different engine performance and emissions parameters further confirmed the repeatability of the tests. For example, Table A1 presents the statistical analysis of the two repeated tests for engine torque, speed and CO_2. As can be seen, the difference between two cold start tests for engine torque, speed and CO_2 were 0.82, 0.02 and 0.12%, respectively, which clearly demonstrate the repeatability of the test. In addition to CO_2 emissions, the repeatability of the engine speed and torque between the tests were also evaluated given that these two parameters can be the indicative of any change in engine operation between the tests.

915

916 Table A1 Test repeatability statistical analysis

		Engine torque (Nm)			Engine speed (rpm)			CO_2 (%)		
		Average	SD	CoV (%)	Average	SD	CoV (%)	Average	SD	CoV (%)
Cold start	Test 1	225.28	8.43	3.74	1498.87	2.22	0.15	6.36	0.06	0.97
	Test 2	227.20	12.32	5.42	1499.19	1.95	0.13	6.51	0.15	2.27
	Difference	0.82%			0.02%			0.12%		
Hot start	Test 1	238.28	3.2	1.34	1498.94	2.20	0.15	6.47	0.03	0.51
	Test 2	242.02	2.42	1.00	1499.49	2.16	0.14	6.64	0.02	0.36
	Difference	1.5%			0.04%			0.17%		

917

918 As a validation step and to show the test-to-test variation and its influence, Figure A1 shows

919 the IMEP and the error bar representing the standard deviation on each experimental points.

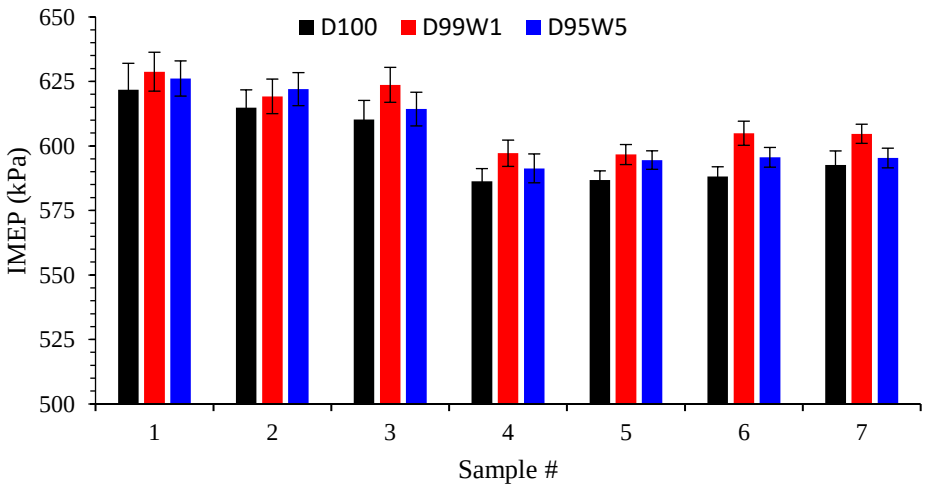

920

921 Figure A1 IMEP within the custom test for all the tested fuels

922